Design and analysis of total internal reflection surface for uniform illumination of incoherent lightings

JU YONG CHO, AND WON KWEON JANG*

[1]*Department of Electric and Electronic Engineering, Hanseo University, 46, Hanseo 1-ro, Seosan-si 31962, South Korea*

Abstract: The design of standard and aspherical optical surfaces often requires time-consuming iterative calculations and relies on point-source assumptions. Consequently, these standard designs are often unsuitable for high-power LEDs with extended emitting areas due to the mismatch between design assumptions and actual source characteristics. In this study, we performed ray tracing simulations to investigate optical efficiency as a function of the light-emitting source size. First, we modeled systems using commercially available surfaces. Under the simulation conditions, maximum power efficiency on a 0.5 mm × 0.5 mm target plane at z = 100 mm decreased from 0.95 to 0.83 as the source width increases from 0.1 mm and 1.4 mm. However, using our proposed strategy optimized for larger emitting areas, the efficiency remained stable, shifting only from 0.93 to 0.91 for the same source widths. Although the proposed model shows a slight reduction in peak efficiency for near-point sources compared to the standard model, it demonstrates significantly higher efficiency and stability for larger light-emitting sources.

Keywords: Optical surface; light emitting diode; optical power efficiency; total internal reflection; ray tracing; optical design simulation

1. Introduction

Light emitting diodes (LEDs) offer numerous advantages over the traditional incandescent lamps, including lower cost, reduced electric power consumption, a longer lifetime, improved stability, and greater environmentally friendliness [1–5]. Consequently, LEDs have found applications in various fields, such as spotlights, streetlights, vehicle headlamps, and medical industry.

LEDs exhibit a Lambertian radiation distribution, which can pose challenges when applied to general lighting systems. This necessitates a specifically designed lighting system, potentially resulting in relatively lower efficiency. The optical design for the LEDs enables the emitted light to be uniform and efficient distribution onto the target illumination surface, fulfilling the necessary requirements for illumination.

Standard conic and aspherical optical surfaces are considered for producing specific distribution by redirecting light rays. Lenses employing multiple conic or aspherical optical elements have been developed based on these candidates [6,7]. However, this design approach often leads to huge volume and inefficiencies in effectively utilizing light rays. Moreover, the assembly of these elements requires strict alignment to achieve optimal performance.

Total internal reflection (TIR) lenses are good substitutes for conventional lenses, designed to optimize light efficiency in LED illumination. Constructed as a unified unit, they offer distinct advantages, such as notably reduced light loss and a more compact form factor.

While a few methods have been proposed to design the TIR freeform lens [8–11], there are some potential issues such as relatively large surface design error. Thus, the determination of the freeform surface in a rigorous manner usually leads to the tedious Monge-Ampere second order nonlinear partial different equation [12,13].

In many applications demanding high-power LEDs, the size of the light sources often increases. When designing TIR surfaces, LEDs are typically treated as point sources, but this simplification can lead to inaccuracies. Since all

optical systems must adhere to etendue restrictions, the TIR surface might not precisely collimate the light emitted from an LED. As a result, adjustments to the TIR surface become necessary. However, optimizing this surface usually requires iterative calculations, which can be a time-consuming process.

In this paper, a straightforward strategy for determining the total internal reflection surface is introduced. Unlike other methods, this approach does not necessitate complex derivations. The design of TIR surface is validated through ray tracing simulations. To optimize surfaces for large emitting areas, Divergence angles were divided into two groups: angles within 30° and angles between 30° and 90°. For angles up to 30°, a spherical surface effectively collimates the light from the LEDs, while for angles between 30° and 90°, collimation is achieved by the total internal reflection surface. The optical efficiency is investigated in terms of various source sizes. Consequently, an optimal size of total internal reflection surface can be determined in relation to the sizes. This method facilitates the creation of an efficient TIR surface suitable for high-power LEDs with larger emitting areas.

2. Methods

Figure 1 illustrates the typical optical design of a TIR lens, accounting for two divergence angle ranges: within 30° and exceeding 30°. In Fig. 1(a), the ray tracing result depicts divergence angles within 30°, where most rays can be regarded as paraxial rays effectively collimated by a spherical surface. However, light with divergence angles larger than 30° is difficult to collimate using conventional optical systems comprised of spherical surfaces, resulting in a significant decrease in optical efficiency. As shown in Fig. 1(b), this large-angle light is effectively collimated by utilizing total internal reflection.

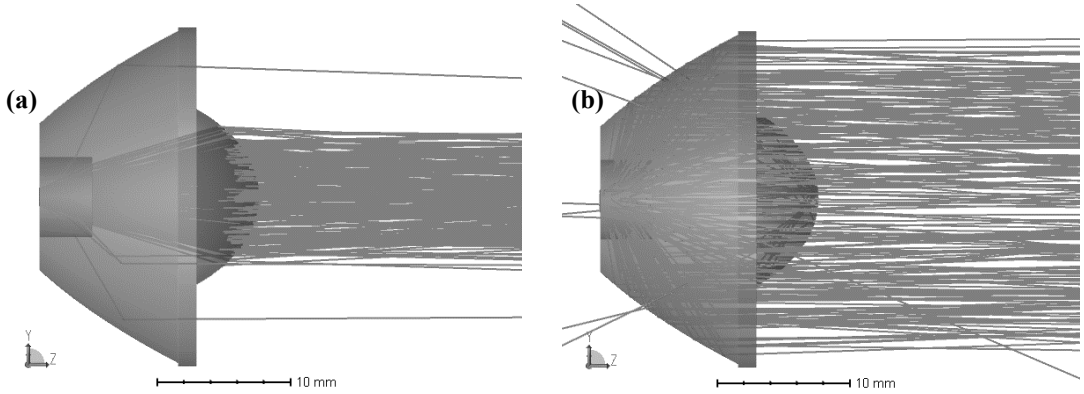

Figure 1. Optical design of total reflection surface: (a) considering divergence angle within 30° and (b) considering divergence angle between 30° and 90°.

Figure 2 shows geometrical analysis of total internal reflection for the light with divergence angles larger than 30°. Light rays propagate through the air and are refracted at the inner surface of the lens in accordance with Snell's law. The position of outer TIR surface can be established using Cartesian coordinates, requiring the definition of an incremental angle $\Delta\theta$. This value can be obtained by dividing the largest angle $\theta_{\max}$, which depends on the divergence angle of an LED, by N elements. The number of N elements should be numerous for precise calculation of the TIR surface.

The coordinates of the refraction point are expressed as a function of the incident angle as follows:

$$r_i(\theta_i) = (x_i, y_i) = (x_0, x_0 \tan\theta_i), \tag{1}$$

where θ_i is incident angle at (x_i, y_i). The refracted light with a refracted angle θ_r travels inside the medium and is then reflected at outer TIR surface. With the position where the light undergoes reflection, the refractive angle θ_r can be calculated by determining the difference between the refraction position and the reflection position. The condition for total reflection is given as follows:

$$n_2 \sin\theta_r = n_1 \sin\theta_c = n_1 \sin\frac{\pi}{2} = n_1, \tag{2}$$

where θ_r is incident angle, which corresponds to the refraction angle at the inner surface, and θ_c is critical angle which is treated as the reflection angle at the outer TIR surface. n_1 and n_2 are refraction indices. Since the light travels the air before refraction, n_1 is 1. Assuming that reflection is specular. The incident angle and the reflection angle must be equal at the outer surface. The angle can be expressed in conjunction with the refractive angle θ_r.

$$\varphi = \varphi' = \frac{\theta_r + (\pi/2)}{2} = \frac{\pi}{4} + \frac{\theta_r}{2} \tag{3}$$

where φ and φ' are the incident angle and the reflection angle, respectively. The intersection point of the ray $R_i(x_i, y_i)$ and the subsequent point of the ray $R_{i+1} = (x_f, y_f)$ composes tangential equation as follows:

$$\frac{y_f - y_i}{x_f - x_i} = \tan\gamma \tag{4}$$

where the point of the ray $R_i = (x_i, y_i)$, the point of the subsequent ray $R_{i+1} = (x_f, y_f)$, the angle γ is equal to θ_r based on Fig. 2. By solving this equation iteratively for each angular step $\Delta\theta$, the continuous profile of the TIR surface is generated, ensuring that light from the extended source region is redirected efficiently.

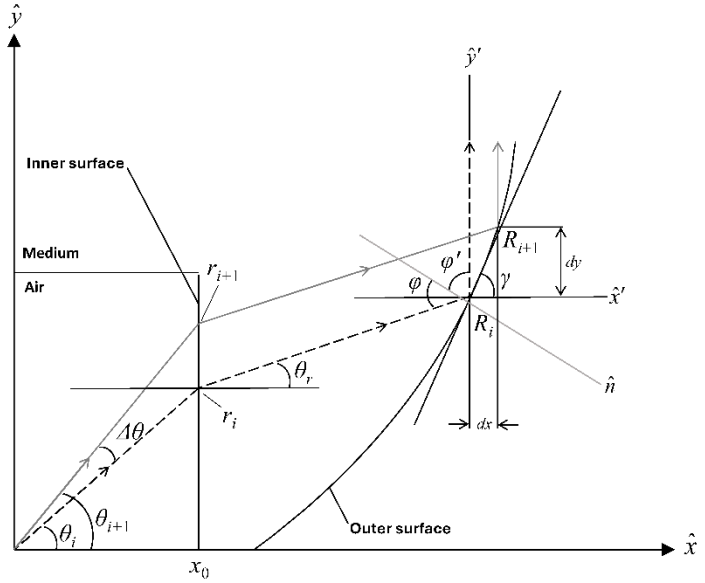

Figure 2. Geometrical analysis of total reflection surface.

3. Results and discussions

To validate the calculation of the total reflection surface, two TIR surfaces are examined, as depicted in Fig. 3. The initial model (grey solid line) is a conceptual representation resembling a commercially available TIR lens. This model was designed under the assumption of a point source. However, when dealing with larger light emitting source sizes, the lens struggles to sufficiently collimate the emitted light, resulting in decreased optical efficiency. Consequently, modifications to the TIR surface become necessary. The overall efficiency is contingent upon the etendue. To preserve a low divergence angle, the TIR surface size needed enlargement, as illustrated in the Modified model (black solid line).

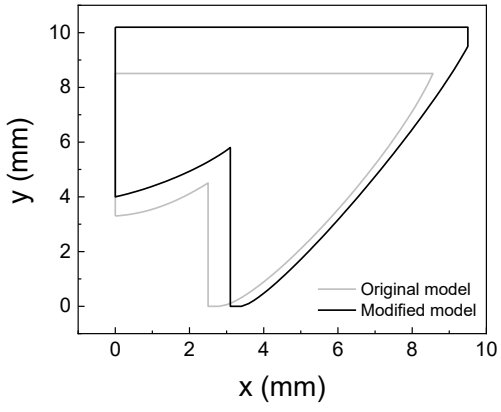

Figure 3. Comparison of total reflection surfaces.

The source width was varied from 0.1 mm to 1.4 mm. A detector plane with dimensions of 25 mm × 25 mm was positioned at a distance of z = 100 mm. The source was modeled with a divergence angle of approximately 140° to

match commercially available LEDs, as shown in Fig. 4. For this simulation, the LED output power was assumed to be 1 W.

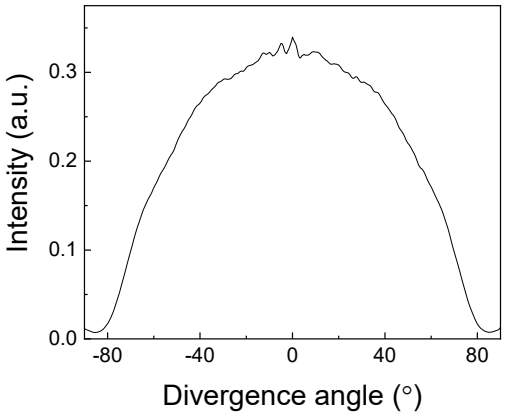

Figure 4. Divergence angle of commercially available LEDs.

The evaluation of the TIR surface was conducted by considering various divergence angles. To collimate all rays emitted from the LED using the TIR surface, the surface area must be enlarged, which inevitably increases the system volume. For optimal performance, rays within a 30° angle are designed to pass through the inner spherical surface, as shown in Fig. 3, while the remaining rays are reflected by the TIR surface.

Figure 5 presents an investigation of optical power relative to source size, specifically for rays within the 30° divergence cone. Although the inner spherical surface was iteratively optimized to collimate rays from the source, adequate collimation was not achievable, as illustrated in Fig. 5(a). Figure 5(b) depicts the optical power efficiency at the illuminated plane. With a source size of 0.1 mm, the efficiency is 0.98 for the Original model and 0.97 for the Modified model. However, with a source width of 1.4 mm, the efficiency drops to 0.56 and 0.80 for the Original and Modified models, respectively."

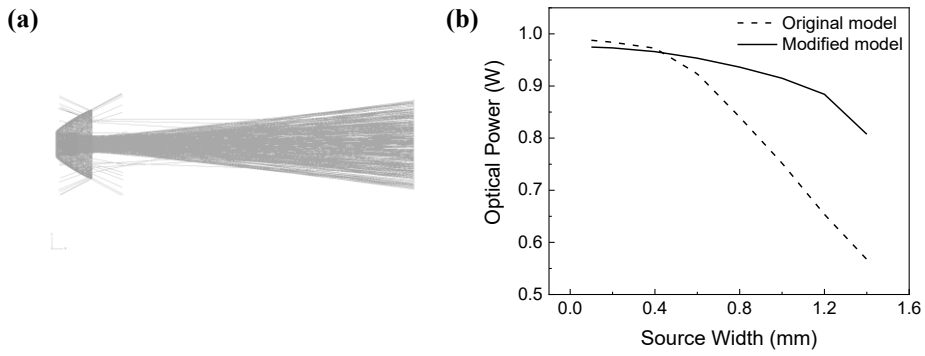

Figure 5. Optical power investigation within a divergence angle of 30°: (a) optical layout and (b) optical power variations with source width.

The rays reflected by the TIR surface were investigated as shown in Fig. 6. Figure 6(a) illustrates the optical layout of the TIR surface for ray angles ranging from 30° to 90°. Unlike the results in Fig. 5(a), collimated rays are clearly evident here. Figure 6(b) presents the optical power efficiency received at the illuminated plane. With a source size of 0.1 mm, the efficiency is 0.94 for the Original model and 0.93 for the Modified model. For the Original model, efficiency decreases to 0.90 when the source size reaches 1.34 mm. In contrast, at a source width of 1.4 mm, the efficiency is 0.89 and 0.92 for the Original and Modified models, respectively.

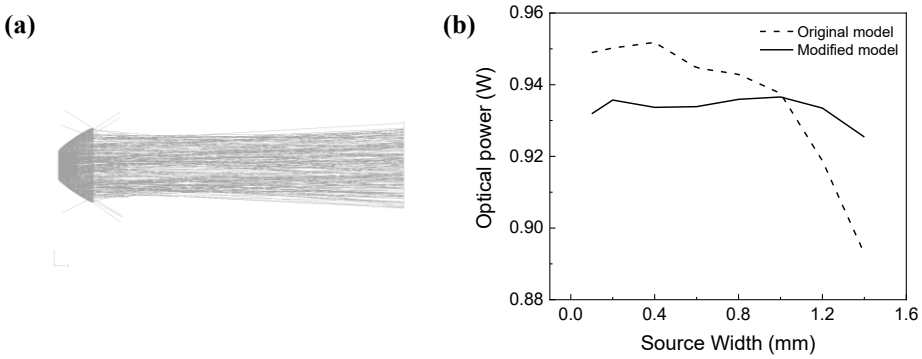

Figure 6. Optical power investigation within a divergence angle range of 30 to 90°: (a) optical layout and (b) optical power variations with source width.

The investigation of rays emitted from the source is presented in Fig. 7. Figure 7(a) shows the optical layout of the TIR surface considering the full angular range. Similar to Fig. 6(a), collimated rays are clearly evident. Figure 7(b) displays the optical power efficiency received at the illuminated plane. For a source size of 0.1 mm, the efficiency is 0.95 for the Original model and 0.93 for the Modified model. However, with a source width of 1.4 mm, the efficiency shifts to 0.83 and 0.91 for the Original and Modified models, respectively. Notably, the Modified model maintains higher efficiency with larger sources. These findings suggest that the Modified model is more suitable for high-power LED applications characterized by large emitting area and large source size.

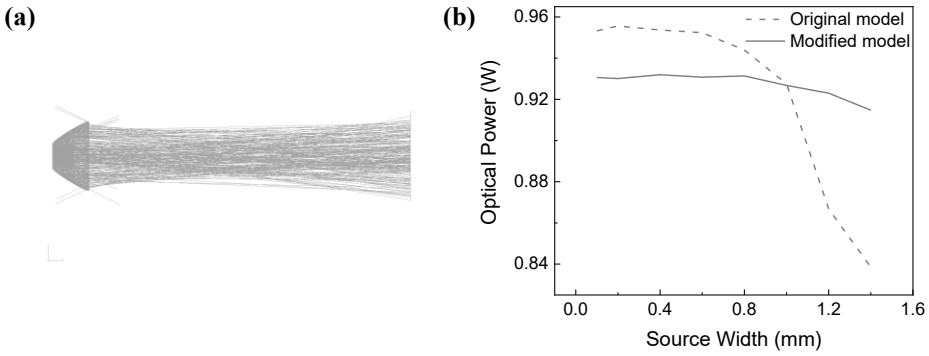

Figure 7. Optical power investigation considering full divergence angle: (a) optical layout and (b) optical power variations with source width.

4. Conclusion

Two TIR surfaces were developed using a streamlined design strategy, serving as an alternative to the complex derivations required for conventional conic and aspheric surfaces. Ray tracing simulations validated these designs by assessing optical efficiency across varying source sizes. The results confirm that to overcome etendue limitations and accommodate larger emitters, the TIR surface must be enlarged. While the Modified model exhibits a slight reduction in optical efficiency compared to standard commercial surfaces for point sources, it provides superior stability and uniformity for extended sources. This design effectively enables uniform illumination for high-power LEDs with large emitting areas.

Disclosures

The authors declare that there are no conflicts of interest related to this article.

Acknowledgements

This work is financially supported by Hanseo university, Seosan, Chungnam, Republic of Korea.

References

1. C. Y. Ho, W. C. Wu, C. S. Chen, C. Ma, and Y. H. Tsai. “Measurement for temperature on a LED lamp,” in 2015 IEEE International Conference on Consumer Electronics - Taiwan, Taipei, Taiwan, Jun. 2015, 282–283.10.1109/ICCE-TW.2015.7216899.
2. D. Gao, X. Ji, W. Pei, X. Zhang, F. Li, Q. Han, and S. Zhang. (2023). “Thermal management and energy efficiency analysis of planar-array LED water-cooling luminaires in vertical farming systems for saffron.” Case Studies in Thermal Engineering. 51. 103535. 10.1016/j.csite.2023.103535.
3. Q. Lin, W. Chunqing, and T. Yanhong. “Thermal design of a LED multi-chip module for automotive headlights,” in 2012 13th International Conference on Electronic Packaging Technology & High Density Packaging, Guilin, Guangxi, China, Aug. 2012, 1435–1438.10.1109/ICEPT-HDP.2012.6474876.
4. G. Patil, S. Kumar, N. Dogra, J. Nindra, S. Kadam, and K. Yadav. (2023). “A comparison of the shear bond strength of metal orthodontic brackets that have been treated with various light-emitting diode intensities and curing times: In-vitro research.” International Journal of Experimental Research and Review. 34 Special Vo: 1–10. 10.52756/ijerr.2023.v34spl.001.
5. X. Yu, P. Zheng, Y. Zou, Z. Ye, T. Wei, J. Lin, L. Guo, H.-G. Yuk, and Q. Zheng. (2023). “A review on recent advances in LED-based non-thermal technique for food safety: current applications and future trends.” Critical Reviews in Food Science and Nutrition. 63 25:. 7692–7707. 10.1080/10408398.2022.2049201.
6. T. Talpur and A. Herkommer (2016), “Review of freeform TIR collimator design methods.” Advanced Optical Technologies. 5 2 :. 137–146. 10.1515/aot-2016-0003
7. J.-J. Chen, T.-Y. Wang, K.-L. Huang, T.-S. Liu, M.-D. Tsai, and C.-T. Lin (2012), “Freeform lens design for Led collimating illumination.” Optics Express. 20 10 :. 10984–10995. 10.1364/OE.20.010984
8. Y.-S. Syu, C.-Y. Wu, and Y.-C. Lee (2019), “Double-Sided Freeform Lens for Light Collimation of Light Emitting Diodes.” Applied Sciences. 9 :. 5452. 10.3390/app9245252.

9. R. Zhu, Q. Hong, H. Zhang, and S.-T. Wu (2015), “Freeform reflectors for architectural lighting.” Optics Express. 23 25:. 31828–31837. 10.1364/OE.23.031828.
10. H. R. Ries, and R. Winston (1994), “Tailored edge-ray reflectors for illumination.” Journal of the Optical Society of America A. 11 4:. 1260–1264. 10.1364/JOSAA.11.001260.
11. J. C. Miñano and J. C. González (1992), “New method of design of nonimaging concentrators.” Applied Optics. 31 16:. 3051–3060. 10.1364/AO.31.003051.
12. H. Ries and J. Muschaweck (2002). “Tailored freeform optical surface.” Journal of the Optical Society of America A. 19 3:. 590–595. 10.1364/JOSAA.19.000590.
13. D. Ma, Z. Feng, and R. Liang (2015). “Freeform illumination lens design using composite ray mapping.” Applied Optics. 54 3 :. 498–503. 10.1364/AO.54.000498.